Seismic Assessment of Tall RC Frames with Hybrid Friction Damper and SMA Designed by PBPD Method

Faramarz Norouzi[1], **Heydar Dashti Naserabadi**[*,2], **Morteza Jamshidi**[3]

[1] *Ph.D student, Department of civil Engineering, Islamic Azad Univerity, Chalus Branch, Chalus , Iran.*

E-mail: f.norouzi@baboliau.ac.ir

[2] *Professor, Department of civil Engineering, Islamic Azad Univerity, Chalus Branch, Chalus , Iran.*

Corresponding Author E-mail: dashti @iauc.ac.ir

[3] *Professor, Department of civil Engineering, Islamic Azad Univerity, Chalus Branch, Chalus , Iran.*

E-mai: m.jamshidi@auc.ac.ir

Abstract. This study, proposes a new lateral load resisting system for high-rise (Reinforced Concrete) RC frames, which includes friction damper-superelastic SMA wires. The proposed SMA-friction damper can not only regulate the mechanism of frictional energy dissipation components with its self-centering SMA wires according to the design method based on the proposed performance, which is able to provide a

hysteretic behavior and high self-centering capacity with the lowest SMA consumption but also has some advantages such as simple configuration and economic application. In this paper, two high-rise 18 and 22-story RC frames were designed in two design modes of common and with the proposed damper. The nonlinear time history analysis subjected to 10 far-field earthquakes performed in Opensees software. The results of the analyses showed that using the proposed SMA-friction damper, in addition to the effective increase in ductility, lateral stiffness and lateral strength, provided an excellent self-centering capacity, which resulted to the significant reduction in the maximum drift and the residual deformations in the structure.

Keywords: RC frames; Nonlinear analysis; Performance-based design; Opensees

1. Introduction

Recently, the seismic design of structures has led to a performance-based approach, where there is a need for new structural members and systems that have increased deformation and flexibility capacity, higher tolerance for damage, and the improvement or reduction of permanent deformations [1-3].

Several studies have been developed and tested for the application of SMAs in civil engineering for devices with self-centering properties and the effectiveness of SMA damping were shown for seismic protection of building structures through numerical and experimental studies [4-6]. The study

conducted by Dorvar et al [7], the effect of changing the hysteresis properties of SMA material which was used as a passive control device in eccentrically bracing frames was investigated. The results showed that the use of the SMA superelastic characteristic provides a great rehabilitation capacity in addition to the effective increase in ductility-stiffness and lateral resistance which results in a significant reduction in terms of both the maximum drift and the residual deformations in the structure. Qian et al [8] investigated a friction damper equipped with SMA under seismic loads. The results showed that an SMA-equipped friction damper under severe earthquakes effectively improved the dynamic response of the structure by dissipating a large portion of the input energy. In addition, with the self-centering capacity of damper, the structure can be reused to withstand subsequent seismic loads without any residual drift [9].

In this research, a device with both the ability of energy dissipation and providing self-centering capacity as a hybrid device is designed. This device is designed for use in high-rise moment resisting frames to improve seismic performance and reduce the residual deformation by using performance-based plastic design methods. The design method is such that, with the greatest contribution to the friction damper in energy dissipation, SMA wires are also at its highest capacity for returning to the initial state of the structure. SMA features are also examined in determining this goal. Finally, nonlinear time history analysis of 18 and 22-story RC frames with or without the proposed hybrid damper is used to examine the expected goals of this type of system for RC structures.

2. Theory

2.1. The Performance of the proposed hybrid friction damper equipped with SMA

The proposed hybrid friction damper (PHFD) acts as a fuse in the structure and by concentrating on non-linear behavior in itself, it prevents non-linear behavior and damage to other structural and non-structural components. The PHFD damper consists of two parts. The first part is a friction damper that works with high seismic energy dissipation through friction between two contact plates, with a perpendicular contact force that can be created through high-strength bolts. Brake pad layers on steel, steel on brass and steel on steel are commonly used as sliding surfaces for this type of damper. The choice of base metal for a friction damper is very important. High corrosion resistance can often reduce the friction reduction coefficient assumed for the life of the device. Low carbon steel alloy rusted and corroded and their sliding surface properties change over time. Experiments on stainless steel in contact with brass did not show any additional corrosion. Therefore, these materials are suitable for use in friction dampers [10]. The motion range of friction dampers is limited by slot holes with slot length equal to S. The value of S is equal to the maximum inter-story drift at the desired performance level. Since the PHFD damper design method is a performance-based approach, the structure for the desired seismic hazard level is designed in such a way that, the inter-story drift is not expected higher than the permissible amount at the performance level. When the displacement reaches the slipping limit of S, the

bolts collides with their end wall, after which further slipping motion will be prevented.

The second part of the PHFD damper consists of a self-centering damper based on the superelastic SMA wires. The superelastic NiTi wires have essentially their self-centering role in addition to large force absorption and hysteric damping properties. With the proper design of the number of superelastic SMA wires stretched appropriately, the device is capable of providing energy dissipation and self-centering capacity, which can reduce the seismic response of the building, leading to the return of the building to the initial conditions after the earthquake. SMA wires are wound around two bars. Each of these two bars has an equal motion range of S in terms of tensile or compressive force that according to Fig. 1, they can move on all three upper, lower and middle steel plates of the right side by creating a slot hole with the length of S. Initially (V=0), the right bar is in contact with the end of the slot hole and the left bar is spaced S to the end of the slot hole. By increasing the force V, which is the sum of the frictional force and the strength of the SMA wires, the left bar remains fixed, and the right rod moves to the right by the length of the SMA wires increase. By further moving of the right middle steel plate, the end of the slot hole collides with the left bar, and eventually, the SMA wires will not be able to extend longer and provide more strength. In this paper, a proposed design method is provided to determine the optimal ratio between SMA wires and frictional force at the PHFD damper. This coincidence method ensures the activity of two dampers in order to provide proper self-centering capacity and energy dissipation equal to seismic demand.

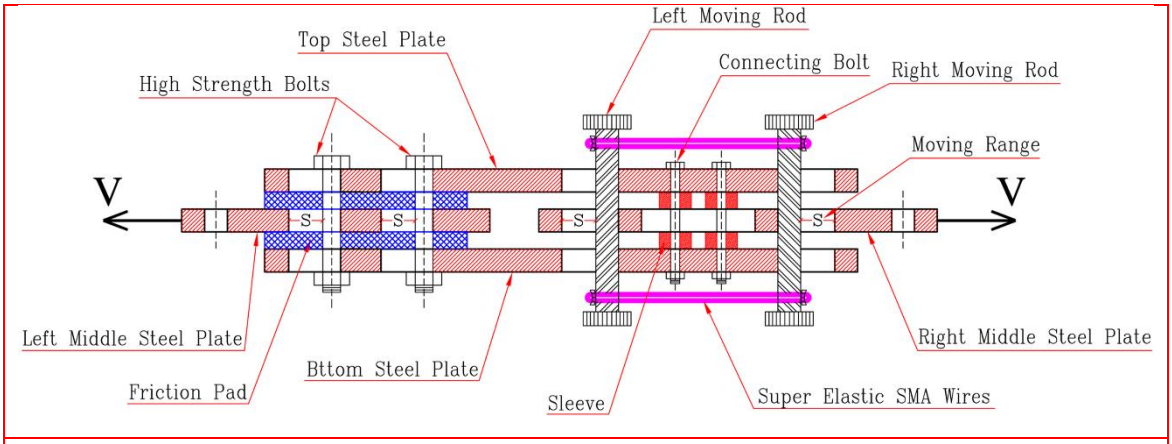

Figure 1: Configuration of the PHFD damper

3. Results and Discussion

3.1. The proposed design method of the RC frame with the PHFD damper

Analytical models in order to evaluate the PHFD damper are two high-rise 18 and 22-story RC frames with a height of 3.80 meters for each floor and with 5 bays of 6 meters in two categories with or without proposed damper. The first group of models includes a special moment resisting frame with the name of SMRF, which was designed at the performance level of life safety according to the latest edition of the earthquake standard and the National Building Code of Iran. The second group of models is RC frames, along with a proposed hybrid damper called PHFD designed according to the proposed design method in this paper. Concrete components of the models were designed in accordance with the ACI 318-08/IBC 2009 codes [11,12]. Materials used in

the frames include concrete with compressive strength and modulus of elasticity, respectively, equal to $f_C = 30$ MPa and $E_C = 28302.4$ MPa, and steel rebars with yield stress and modulus of elasticity of $f_y = 400$ MPa and $E_S = 200000$ MPa. For gravity loading of frames, the design dead load and the live load are considered to be $34.5\ {}^{kN}/_{m}$ and $18.0\ {}^{kN}/_{m}$, respectively. Frame mass in accordance with the ASCE41-06 code is considered to be $1287\ {}^{kN}/_{Floor}$ because of the dead weight of all structural and non-structural components and part of the live load. The structural details of the frames have been shown in Table 1. Also, the elevation of the models has been shown in Figure 2.

Table 1. Specifications of concrete sections for designing the beam and column members

Section	Height (mm)	Width (mm)	Reinforcement*	
			Top Steel	Bottom Steel
B50x50	500	500	4φ25	3φ20
B50x60	500	600	4φ25	3φ25
B50x65	500	650	5φ25	4φ25
B50x70	500	700	6φ25	4φ25
C50	500	500	20φ20	
C55	550	550	24φ22	
C60	600	600	24φ25	
C65	650	650	24φ25	
C70	700	700	24φ28	
C75	750	750	24φ28	

C80	800	800	28φ28
C85	850	850	32φ28

* Number of reinforcements φ Diameter (in millimeters)

The non-yield members are designed with the yielding of the PHFD damper members, taking into account the factor of $1.25\ R_y$ (similar to EBF design in AISC341-10 [13] where Ry is the ratio of the expected yield stress to the lowest yield stress. In the range of unstable buckling of the compressive braces, the tensile and compressive forces are twice the buckling load(P_b). As a result, in order to prevent the unstable buckling of the compressive braces, the sum of horizontal components of the buckling loads of both braces should be higher than the shear required to design the proposed hybrid friction dampers multiplied by $1.25\ R_y$. Where R_y for the sections made of the plate is equal to 1.15 [13]. Thus:

$$2P_b\ Cos\alpha\ \geq\ 1.25\ R_yV \tag{1}$$

In Eq. (19), α is the angle of the brace with the horizon. By solving Eq (1) in terms of the buckling strength of the braces, (P_b) is obtained as Eq. (2).

$$P_b = \frac{1.25\ R_y\ V}{2Cos\alpha} \tag{2}$$

The braces are chosen in such a way that have a minimum computational buckling capacity(P_b). Selected braces with the section of 2UNP120 with buckling strength of 996 KN are responsive for all models.

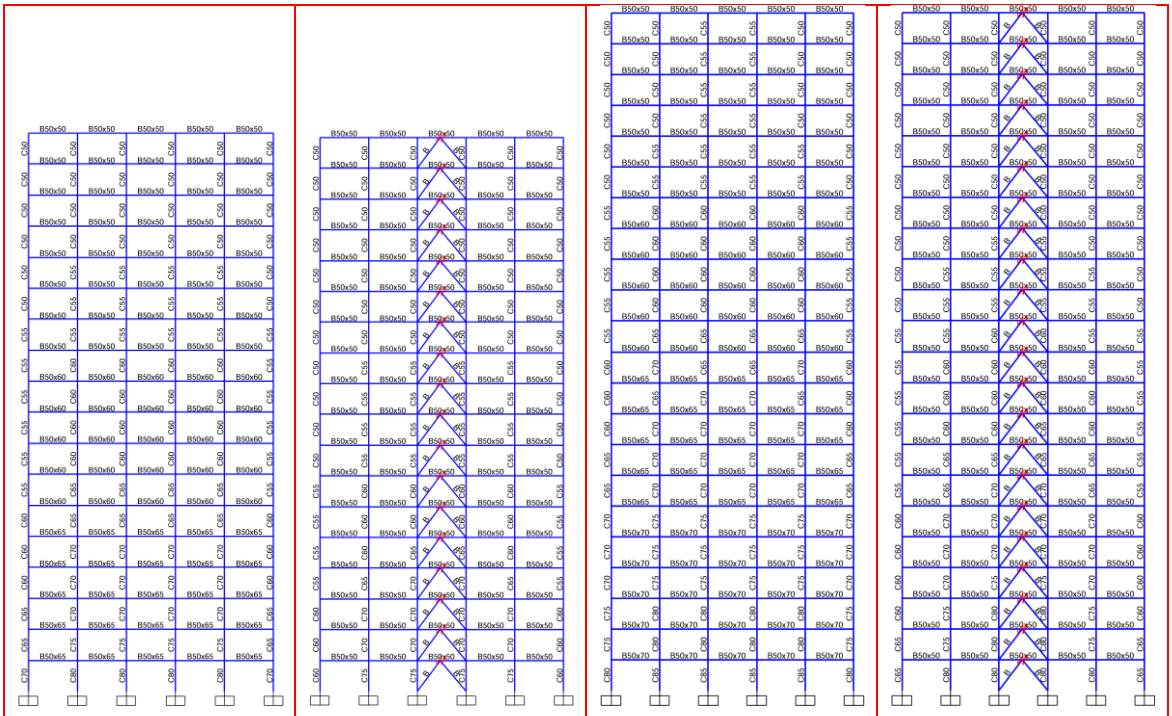

18st- SMRF	18st- PHFD	22st- SMRF	22st- PHFD

Figure 2: Design details of the beam and concrete columns of the used models

3.2. The proposed design method of the RC frame with the PHFD damper

The numerical models of the frames were made using the 2D modeling capability of OpenSees [14]. An axial column carrying gravity load is

connected to the frame to simulate the P-Delta effects. The axial column with an elastic beam-column element with a large cross-section and large inertia moment is modeled to take into account the effect of gravity columns on the overall response of the frame. The beam-column elements in the gravity column are connected to each other by rotational springs with very small rotational rigidity, to ensure that the gravity column does not bear any significant moments. Finally, the gravity column is attached to the frame by truss elements which are quite rigid. The first story columns in the base level for the frame and gravity column are fixed and pinned respectively.

All nodes of a given floor are constrained to the displacement in a horizontal plane, which simulates a rigid diaphragm. The seismic mass of each floor is distributed equally between the beam-column nodes. Gravity loads, which is direct loading of the frame are applied to the frame beam-column nodes and also to the gravity column to take into account the P-Delta effects for the frame. The damping assigned to the elements and nodes is modeled by the Rayleigh command in the software. Zerolength element with high rigidity was only used in the transmission direction in order to model the rotational connection at the junction of braces to the beam and the column. The used materials were chosen from the uniaxial material model which are able to consider the interaction between the axial and the moment forces with the ability to generate a one-dimensional stress-strain relationship. The concrete material model, including confined and unconfined concrete of Concrete 02 type, and steel model of Steel02 type are defined in the OpenSees software. The beam, columns and braces members have been modeled with the nonlinear beam-column element

with broad plasticity and are divided into five sections. The integral points of the element direction are based on the quadrature Gauss-Lobatto law. All sections were modeled with the Fiber model. According to FEMAP696 [15], the flexural cracking coefficients of 0.5 and 0.7 were applied in nonlinear analyzes for concrete beam and columns. For this purpose, two concrete materials were defined for the beam and column in which the modulus of elasticity multiplied by 0.5 and 0.7.

To describe the numerical model of SMA wires, uniaxial self-centering materials were used. This flag-shaped material is capable of describing a superelastic behavior of shape memory alloy at a constant temperature. For simplicity, Steel 01 materials with hardening of close to zero, which represents the elastic-perfectly plastic model, are used for friction damper models. Each part of the PHFD damper is modeled with the above mentioned materials and combined with uniaxial parallel materials that lead to simultaneous operation. Finally, it is simulated with a Zero-Length element above the Chevron brace and below the concrete beam.

4. Discussion

4.1. Analysis of Nonlinear time history

In this section, a comprehensive study on two-dimensional dynamic nonlinear time history analysis conducted by OpenSees is carried out to identify the seismic behavior of high-rise 18 and 22-story RC frames in two modes: (1) Designed in accordance with the current methodology in the Codes and, (2) designed with the PBPD method along with the PHFD damper. The focus is on two commonly used quantities: inter-story drift ratio (IDR) and

residual drift ratio (RDR) for each story, so that in addition to judging the seismic performance of structures during earthquakes, it is possible to identify and study the stories with the maximum IDR and RDR. The IDR is used to express the overall stability of RC frames under earthquakes. Also, the two above-mentioned quantities are capable of providing an appropriate measurement for the evaluation of damages to structural and non-structural components due to seismic loading.

First, the frames are subjected to 10 earthquakes. These earthquakes are representative of the DBE level earthquake excitations (the probability of incidence of 2% over a period of 50 years) and the MCE level earthquake excitations (the probability of incidence of 10% over a period of 50 years). Figure 3 shows the maximum IDR with their mean values for 18 and 22-story frames with and without the PHFD dampers as a function of the NLTH analysis of 10 earthquakes, for assessing each performance level. The frames with PHFD damper provide a better response than conventional frames at both levels of performance. In addition, regardless of the characteristics of earthquakes (such as the content frequency) used in the analysis, it has a much more stable response, i.e. a more uniform or similar response to all selected earthquakes. In conventional frames (SMRF), drift distribution occurs at the height of the structure irregularly and the maximum IDR occurred in the upper stories due to the whipping force of the earthquake, because in the conventional design of RC frames, it is expected that the beams and especially the columns in the lower stories have weaker sections due to the lower gravity loads. Hence, during earthquakes and the dominance of higher modes in the maximum

structural deformation, the end stories with the maximum IDR subject the structures to rupture. However, in the case of using the PHFD damper, developed by the PBPD, makes this weakness an opportunity for the participation of all stories to counter the earthquake's lateral force. In these models, the change in maximum IDR is increased from base story to third and by moving to the roof, its amount is reduced, so that, as we get closer to the roof, the difference between the IDR values is reduced, and the IDR values are approximately identical from the midpoint of the height of the structure to the roof. This result shows that the design is based on performance for the RC frame with the PHFD damper by considering the effects of the interaction according to the proposed method which leads to the design of a lateral load resistance system by providing a behavior close to the ideal during earthquake events.

The mean of maximum IDR in frames with PHFD damper have shown a more uniform distribution at the height of the frames, and a significant reduction in different story levels compared to the main frame. The reduction of the mean of maximum IDR at different levels of the 18 and 22-story frames in the case with a PHFD damper compared to the main case at the LS performance level was 69.8% and 57.9% respectively, and at CP level was 67.7% and 56.6% respectively. By increasing the number of stories of the models from 18 to 22, the reduction of the mean of maximum IDR decreases. Also, with the increase in the intensity of earthquakes from the DBE to the MCE level, the reduction of the mean of maximum IDR decreases insignificantly, which can be neglected. As it is known, in the case of using RC frames with the PHFD

damper, regardless of the number of stories and seismic intensity, it can reduce the mean of maximum IDR by about 55-70%. The above result indicates the large absorption of lateral force by the PHFD damper due to the combination of friction dampers with large and stable hysteresis loops and a large elastic stiffness SMA wire set along with large flange-shaped hysteresis loops, which resulted in the provision of a system with large lateral stiffness and force dissipation.

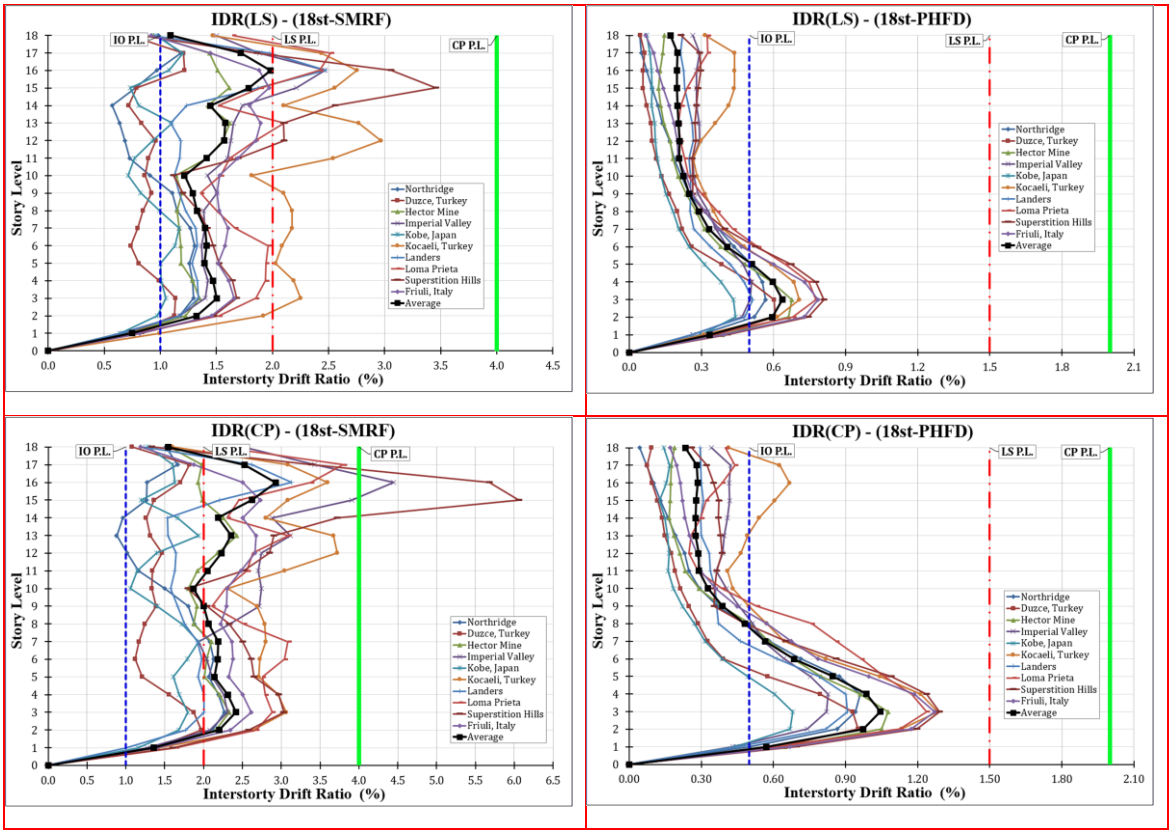

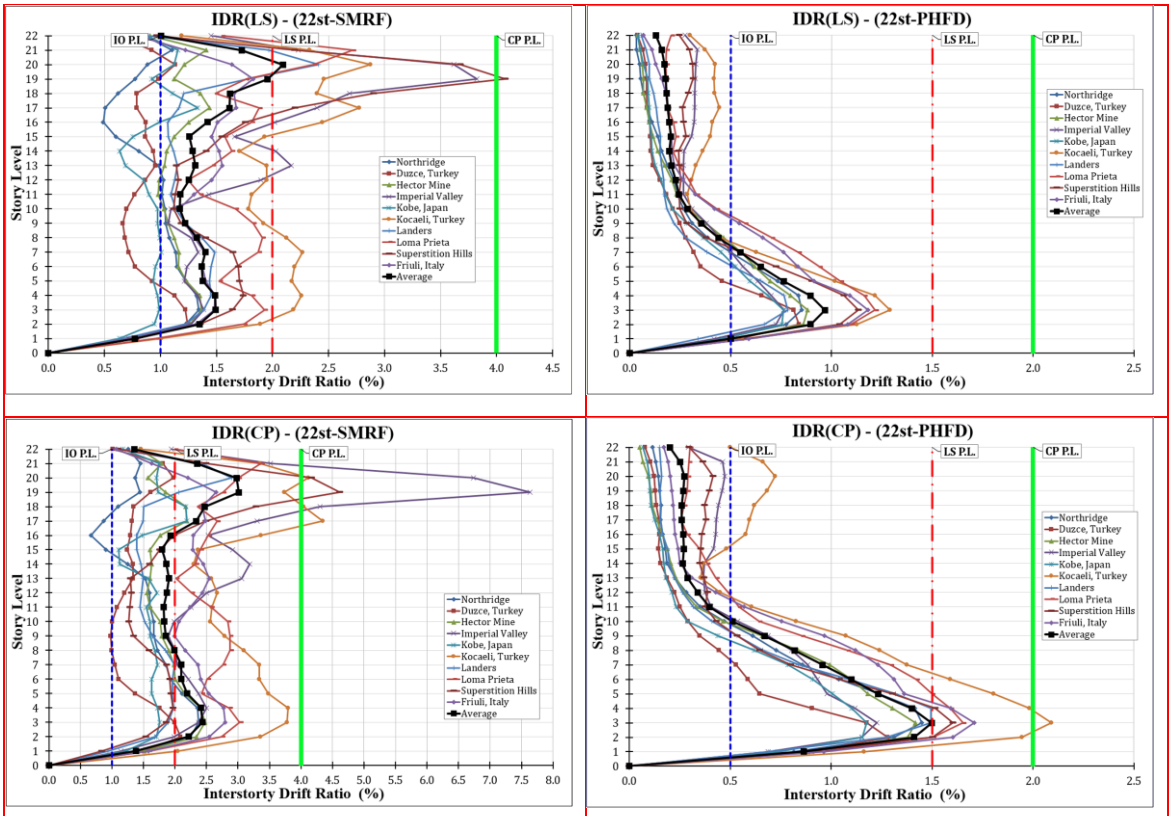

Figure 3 The performance comparison of eccentrically braced frames with and without PHFD damper in terms of IDR at the LS and CP performance levels

The structural performance of the models was evaluated in accordance with ASCE standard 41-06 and summarized in Tables 2 and 3. Structural performance based on IDR and RDR was considered. Based on ASCE 41-06 standard in SMRF models, when IDR is less than 1.0%, between 1.0-2.0 %, more than 2.0% and also when RDR is 0.0%, between 0.0-1.0%, more than 1.0%, the structural performance levels are respectively equal to immediate occupancy (IO), life safety (LS) and collapse prevention (CP).In PHFD models, when the IDR is less than 0.5%, between 0.5-1.5%, more than 1.5% and also

when RDR is 0.0%, between 0.0-0.5%, higher than 0.5%, the structural performance levels are respectively equal to IO, LS, and CP. As shown in Table 5, the structural performance level of the 18st-SRMF, 18st-PHFD, 22st-SRMF and 22st-PHFD models for the IDR of DBE seismic level respectively include (LS 50%, CP 50%), (LS 100%, CP 0%), (LS 50%, CP 50%) and (LS 100%, CP 0%) and at the seismic level of the MCE include (LS 20%, CP 80%), (LS 100%, CP 0%), (LS 0%, CP 100%) and (LS 60%, CP 40%). It has been found that ordinary RC frames at the seismic level of DBE provided 50% of appropriate structural performance level, while the RC frames with the PHFD dampers provided 100% of it. Also at the seismic level of MCE, the appropriate structural performance level for RC frames without and with PHFD damper are equal to 0-20% and 60-100% respectively.

Table 2: The Structural performance level of models subjected to 10 earthquakes for the IDR ratio

Ground motions	18st-SMRF				18st-PHFD				22st-SMRF				22st-PHFD			
	DBE Level		MCE Level		DBE Level		MCE Level		DBE Level		MCE Level		DBE Level		MCE Level	
	IDR (%)	S.P. level	IDR (%)	S.P. level	IDR (%)	S.P. level	IDR (%)	S.P. level	IDR (%)	S.P. level	IDR (%)	S.P. level	IDR (%)	S.P. level	IDR (%)	S.P. level
Northridge	1.30	LS	2.27	CP	0.57	LS	0.96	LS	1.34	LS	2.37	CP	0.85	LS	1.45	LS
Duzce, Turkey	1.22	LS	1.97	LS	0.61	LS	0.95	LS	1.24	LS	2.09	CP	0.84	LS	1.28	LS
Hector Mine	1.62	LS	2.42	CP	0.68	LS	1.08	LS	1.44	LS	2.48	CP	0.88	LS	1.42	LS
Imperial Valley	2.47	CP	4.45	CP	0.51	LS	0.83	LS	3.82	CP	7.63	CP	0.77	LS	1.23	LS
Kobe, Japan	1.20	LS	1.94	LS	0.44	IO	0.68	LS	1.33	LS	2.19	CP	0.76	LS	1.18	LS
Kocaeli, Turkey	2.97	CP	3.72	CP	0.71	LS	1.28	LS	2.87	CP	4.34	CP	1.29	LS	2.09	CP
Landers	2.47	CP	3.13	CP	0.51	LS	0.91	LS	2.41	CP	2.90	CP	0.78	LS	1.49	LS

Loma Prieta	2.52	CP	3.80	CP	0.78	LS	1.24	LS	2.72	CP	3.37	CP	1.22	LS	1.65	CP
Superstition Hills	3.45	CP	6.06	CP	0.81	LS	1.29	LS	4.07	CP	4.62	CP	1.13	LS	1.60	CP
Friuli, Italy	1.97	LS	2.73	CP	0.79	LS	1.27	LS	1.83	LS	2.80	CP	1.18	LS	1.71	CP

Table3: Structural performance level of models subjected to 10 earthquakes for the IDR ratio

Ground motions	18st-SMRF				18st-PHFD				22st-SMRF				22st-PHFD			
	DBE Level		MCE Level		DBE Level		MCE Level		DBE Level		MCE Level		DBE Level		MCE Level	
	IDR (%)	S.P. level	IDR (%)	S.P. level	IDR (%)	S.P. level	IDR (%)	S.P. level	IDR (%)	S.P. level	IDR (%)	S.P. level	IDR (%)	S.P. level	IDR (%)	S.P. level
Northridge	1.30	LS	2.27	CP	0.57	LS	0.96	LS	1.34	LS	2.37	CP	0.85	LS	1.45	LS
Duzce, Turkey	1.22	LS	1.97	LS	0.61	LS	0.95	LS	1.24	LS	2.09	CP	0.84	LS	1.28	LS
Hector Mine	1.62	LS	2.42	CP	0.68	LS	1.08	LS	1.44	LS	2.48	CP	0.88	LS	1.42	LS
Imperial Valley	2.47	CP	4.45	CP	0.51	LS	0.83	LS	3.82	CP	7.63	CP	0.77	LS	1.23	LS
Kobe, Japan	1.20	LS	1.94	LS	0.44	IO	0.68	LS	1.33	LS	2.19	CP	0.76	LS	1.18	LS
Kocaeli, Turkey	2.97	CP	3.72	CP	0.71	LS	1.28	LS	2.87	CP	4.34	CP	1.29	LS	2.09	CP
Landers	2.47	CP	3.13	CP	0.51	LS	0.91	LS	2.41	CP	2.90	CP	0.78	LS	1.49	LS
Loma Prieta	2.52	CP	3.80	CP	0.78	LS	1.24	LS	2.72	CP	3.37	CP	1.22	LS	1.65	CP
Superstition Hills	3.45	CP	6.06	CP	0.81	LS	1.29	LS	4.07	CP	4.62	CP	1.13	LS	1.60	CP
Friuli, Italy	1.97	LS	2.73	CP	0.79	LS	1.27	LS	1.83	LS	2.80	CP	1.18	LS	1.71	CP

The structural performance level of the 18st-SRMF, 18st-PHFD, 22st-SRMF and 22st-PHFD models for the RDR ratio at the DBE seismic level included (LS 90%, CP 10%), (LS 100%, CP 0%), (LS 70%, CP 30%), (LS 100%, CP 0%), and at the MCE seismic level included (LS 60%, CP 40%) (LS 100%, CP 0%), (LS 80%, CP 20%), (LS 100%, CP 0%). The RC frames with PHFD damper provided 100% of the desired structural performance level for all

models and seismic levels. Although ordinary RC frames at the seismic level of DBE provide 70-90% and at the seismic level of MCE provides 60-80% of structural performance, but by leaving the residual drift more than 0.5%, it actually puts the structure in undesirable conditions in terms of dealing with subsequent earthquakes.

Table 4: Structural performance level of models subjected to 10 earthquakes for RDR ratio

Ground motions	18st-SMRF				18st-PHFD				22st-SMRF				22st-PHFD			
	DBE Level		MCE Level		DBE Level		MCE Level		DBE Level		MCE Level		DBE Level		MCE Level	
	RDR (%)	S.P. level	RDR (%)	S.P. level	RDR (%)	S.P. level	RDR (%)	S.P. level	RDR (%)	S.P. level	RDR (%)	S.P. level	RDR (%)	S.P. level	RDR (%)	S.P. level
Northridge	0.31	LS	0.47	LS	0.04	LS	0.03	LS	0.25	LS	0.33	LS	0.04	LS	0.06	LS
Duzce, Turkey	0.15	LS	0.22	LS	0.01	LS	0.03	LS	0.09	LS	0.38	LS	0.04	LS	0.04	LS
Hector Mine	0.30	LS	0.24	LS	0.01	LS	0.02	LS	0.17	LS	0.21	LS	0.03	LS	0.07	LS
Imperial Valley	0.35	LS	1.39	CP	0.01	LS	0.02	LS	1.23	CP	0.54	LS	0.04	LS	0.07	LS
Kobe, Japan	0.12	LS	0.25	LS	0.02	LS	0.01	LS	0.19	LS	0.18	LS	0.01	LS	0.04	LS
Kocaeli, Turkey	0.94	LS	1.33	CP	0.08	LS	0.08	LS	1.95	CP	2.38	CP	0.16	LS	0.19	LS
Landers	1.16	CP	1.13	CP	0.05	LS	0.12	LS	0.52	LS	0.61	LS	0.08	LS	0.17	LS
Loma Prieta	0.25	LS	0.37	LS	0.01	LS	0.02	LS	0.16	LS	0.35	LS	0.02	LS	0.03	LS
Superstition Hills	0.74	LS	1.02	CP	0.02	LS	0.04	LS	1.05	CP	1.18	CP	0.03	LS	0.04	LS
Friuli, Italy	0.29	LS	0.47	LS	0.03	LS	0.04	LS	0.30	LS	0.56	LS	0.01	LS	0.02	LS

5. Conclusion

In this research, the effect of a hybrid friction damper equipped with SMA wire

on reducing the seismic response of high-rise RC frames was investigated. For this purpose, two high-rise 18- and 22-story RC structures with or without PHFD dampers were designed according to the performance-based plastic design method, by considering the interaction effects between the RC frame and the PHFD damper. The comparative study of models by time history analyzing of 10 far-field earthquakes clearly showed the reduction of all important indicators including the inter-story drift ratio (IDR) and the inter-story residual drift ratio (RDR). The average IDR of RC frames with PHFD damper is less than that of conventional RC frames by 55-70% and the IDR distribution at the height of the frames has a more uniform behavior. When the proposed design method based on performance is done considering the proposed limitation for SMA wires (strain less than 6% for determining the length and strain equal to the reversed deformation yield strain for an optimal mechanism with friction damper), RC frames with PHFD damper provide an appropriate reversibility capacity in addition to the maximum energy dissipation capacity, as a result, the average maximum RDR in the case of using PHFD damper in RC frames can be significantly reduced by about 82-97% compared to conventional RC frames. The results of this paper indicate that the proposed damper can bring the RC frame to the structural performance with the least cost and number of bracing spans.

References

[1] Constantinou MC, Soong TT, Dargush GF. Passive energy dissipation systems fro structural design and retrofit. Buffalo (NY): Research Foundation of the State University of New York and Multidisciplinary Center for Earthquake Engineering Research; 1998.

[2] Gao, Y., Ren, W. Theoretical Study on Vibration Control of Symmetric Structure with Shape Memory Alloy (SMA)-Friction Damper", The Open Mechanical Engineering Journal, 8: 803-808, 2014.

[3] Ozbulut, O.E., Hurlebaus, S. (2012). "Application of an SMA-based hybrid control device to 20-story nonlinear benchmark building", Journal of Earthquake Engng Struct. Dyn, DOI: 10.1002/eqe.2160.

[4] McCormick J, DesRoches R, Fugazza D , Auricchio F, Seismic assessment of concentrically braced steel frames with shape memory alloys braces J. Struct. Eng. 133 862–70, 2007.

[5] Asgarian B, Salari N and Saadati B, Application of intelligent passive devices based on shape memory alloys in seismic control of structures Structures 5: 161–169, 2016.

[6] Parulekar Y M et al , Seismic response attenuation of structures using shape memory alloy dampers Struct. Control Health Monit. 19: 102–119, 2012.

[7] Massah ,S.R., Dorvar , H. Design and analysis of eccentrically braced steel frames with vertical links using shape memory alloys, Journal of Smart Materials and Structures, 23: 2014.

[8] DesRoches, R. and Delemont, M. Seismic retrofit of simply supported bridges using shape memory alloy. Journal of Engineering Structures, 24: 325-332, 2002.

[9] Sharabash, A. M. andrawes, B. Application of shape memory alloy dampers in the seismic control of cable-stayed bridge. Journal of Engineering Structures. 31: 607-616, 2009.

[10] Le C.H., Kim J., Kim D.H., Ryu, J., Ju Y.K. Numerical and experimental analysis of combined behavior of sheartype friction damper and non-uniform strip damper for multi-level seismic protection", Journal of Engineering Structures, 114:75-92, 2016.

[11] ACI Standard (ACI 318-08), American Concrete Institute, Building Code Requirements for Structural Concrete and Commentary, Edition January 2008.

[12] IBC: International building code. International Code Council, Inc (formerly BOCA, ICBO and SBCCI) 2009; p. 60478-5795.

[13] AISC 341–10. Seismic Provisions for Structural Steel Buildings, (ANSI/AISC 341–10); 2010.

[14] Pacific Earthquake Engineering research Center. *OpenSees, Open System for Earthquake Engineering Simulation*. (2015-Last update), [Online]. Available: http://opensees.berkeley.edu [2012, Feb. 16]

[15] FEMA. Quantification of building seismic performance factors. FEMA Rep. No. P695, Applied Technology Council for FEMA, Washington, DC; 2009.